Journal of Chromatography A 1777 (2026) 466941

Contents lists available at ScienceDirect

Journal of Chromatography A

journal homepage: www.elsevier.com/locate/chroma

2D-TLC–UV/Vis/FLD–direct bioautography–HRMS/MS-based identification of antibacterial compounds of *Myrtus communis* L

Ecesu Sezen [a], Ágnes M. Móricz [b,*], Péter G. Ott [b], Etil Guzelmeric [a]

[a] Yeditepe University, Faculty of Pharmacy, Department of Pharmacognosy, Istanbul, Türkiye
[b] Plant Protection Institute, Centre for Agricultural Research, Hungarian Research Network, Budapest, Hungary

ARTICLE INFO

Keywords:
Myrtus communis L. (myrtle)
2D-TLC–direct bioautography
2D-TLC–*Bacillus subtilis* assay–tandem high-resolution mass spectrometry
Antimicrobial activity
Myrtucommulones, Triterpenes

ABSTRACT

The search for new antibacterial agents is often hindered by the limited efficiency of traditional isolation-based workflows, which may result in low yields or insufficient detection of bioactive constituents. To address these limitations, an affordable two-dimensional thin-layer chromatography (2D-TLC) combined with direct bioautography was applied for the rapid screening of the hydroalcoholic leaf extract of *Myrtus communis*. The 2D-TLC–UV/Vis/FLD–*Bacillus subtilis* assay provided improved separation capacity, including in overloaded conditions, also enabling the visualization of minor antibacterial zones. Bioactivity-guided HRMS/MS analysis performed directly from the inhibition areas allowed the tentative identification of several triterpenoids and fifteen myrtucommulone-type non-prenylated acylphloroglucinol derivatives. Some of these metabolites have not been previously described in the context of antibacterial screening of *M. communis*. This is the first application of an eight-dimensional workflow integrating 2D-TLC–UV/Vis/FLD–*B. subtilis* bioassay–HESI-HRMS/MS for the screening and characterization of antibacterials in a complex matrix, exemplified here for *M. communis*, which provided previously unexplored compounds with potent antibacterial activity.

1. Introduction

Myrtus communis L. (myrtle, family Myrtaceae), or myrtle, is an evergreen shrub native to the Mediterranean, valued for its medicinal and ornamental uses [1]. Traditionally symbolizing immortality [2], its fruits, leaves, essential oil, and flowers have been used in folk medicine for various ailments, including hypotension, diabetes, inflammation, and gastrointestinal disorders [3].

Scientific studies confirm that *M. communis* exhibits anti-inflammatory, antioxidant, antimicrobial, antidiabetic, anticancer, and hepatoprotective activities [4]. Guzelmeric et al. [5] found that its leaves, rich in myricitrin, showed the strongest antimutagenic and anticancer effects against HT-29 cells (IC_{50} = 8.2 μg/mL). Phytochemically, *M. communis* contains flavonoids, tannins, terpenes, and phloroglucinol derivatives, like myrtucommulones [6]. Myrtucommulones, non-prenylated acylphloroglucinols, represent key bioactive constituents with notable pharmacological effects [7,8]. Appendino et al. [9] demonstrated the antibacterial activity of semimyrtucommulone and myrtucommulone A, isolated from myrtle leaf extract. Tested against multidrug-resistant *Staphylococcus aureus*, myrtucommulone A showed potent activity (MIC 0.5–2 μg/mL), comparable to tetracycline, while semimyrtucommulone was less effective (MIC 32–64 μg/mL). These results highlight the potential of myrtucommulone derivatives as candidates against antibiotic-resistant strains.

To date, studies on *M. communis* have primarily focused on isolating and evaluating its bioactive compounds. However, challenges such as low yield or lack of desired activity in isolated constituents often arise. These limitations highlight the need for rapid, specific, and cost-effective screening methods for bioactives in complex natural matrices.

Thin-layer chromatography (TLC) combined with direct bioautography is an efficient method for affordable, high-throughput, and rapid detection of bioactive compounds in multicomponent samples, such as plant extracts [10,11]. To achieve better separation and lower limit of detection (LOD), high-performance thin-layer chromatography (HPTLC) with finer particle size, automated multiple development [12], two-dimensional (2D)-(HP)TLC [13,14], or forced flow layer chromatographic technique, like overpressured layer chromatography [15] can be used. These techniques significantly increase resolving power and peak capacity, benefits that can be exploited to improve accompanying bioassays. Following a non-target bioautographic screening step, targeted characterization and identification of bioactive compounds is a reasonable option. Qualitative analysis can be performed using various

* Corresponding author.
E-mail address: moricz.agnes@atk.hun-ren.hu (Á.M. Móricz).

https://doi.org/10.1016/j.chroma.2026.466941
Received 16 January 2026; Received in revised form 25 March 2026; Accepted 26 March 2026
Available online 27 March 2026

hyphenated techniques: *in situ* (HP)TLC coupled with Fourier-transform infrared spectroscopy (FTIR) [16] or surface-enhanced Raman spectroscopy (SERS)-FT-Raman [17], or *ex situ* analysis after elution of the target zone by attenuated total reflectance-FTIR (ATR-FTIR) [18] or nuclear magnetic resonance (NMR) spectroscopy [19,20]. However, (HP)TLC hyphenated with UV/Vis/fluorescence detection (FLD)/mass spectrometry (MS) is the most widely used approach for comprehensive characterization. (HP)TLC coupled with MS using desorption-based interfaces like direct analysis in real-time mass spectrometry (DART-MS) [21,22] and desorption electrospray ionization mass spectrometry (DESI-MS) [23] allows for whole-track scanning. Alternatively, the common elution head-based approach involves eluting a 4 mm x 2 mm spot and directly transferring it to the MS [22,24,25]. A native chromatogram, run in parallel with the bioautogram, is typically used for MS analysis of compounds in the bioactive zone [21,22,24,25]. This targeted elution strategy minimizes matrix interference originating from the bioassay medium, and enables selective interrogation of antibacterial zones rather than the entire chemical profile of the extract. Using DART-MS to scan bioautograms (chromatograms dipped in cell suspension and optionally visualized with dye) has been successful in characterizing separated bioactive compounds by the discrimination of polar bioassay ions [26]. However, compared to native chromatograms, the LOD increased fivefold due to the complexity of the cell suspension. Direct (HP)TLC–bioassay–MS hyphenation, using a zone-eluting interface, targets only antibacterial zones with low cell numbers to minimize MS contamination [27].

High MS background intensity (total ion current, TIC) deriving from the bioassay matrix can be mitigated by using buffer-free bioassay media, non-aqueous solvents for elution, negative ionization (where applicable), and/or desalting via eluent split-off during the short initial stages of elution [27–29].

Accordingly, this study was designed based on the hypothesis that improving chromatographic separation using 2D-TLC and combining it with hyphenated analytical techniques provides a rapid and practical approach for the tentative identification of compounds and compound classes potentially responsible for bioactivity in chemically complex plant extracts. The current study aims to screen and characterize antibacterial compounds from the hydroalcoholic extract of myrtle leaves against *B. subtilis* by 2D-TLC–UV/Vis/FLD–direct bioautography coupled with tandem high-resolution mass spectrometry (HRMS/MS).

2. Materials and methods

2.1. Chemicals

Thin-layer chromatography (TLC) plates were obtained from Merck (Darmstadt, Germany, Cat. No. 1.05554.0001). Analytical grade toluene, ethyl acetate, isopropyl acetate, ethanol, and methanol were purchased from Molar Chemicals (Halásztelek, Hungary) or Sigma-Aldrich (St. Louis, MO, USA). Analytical grade acetic acid was obtained from Lach-Ner (Neratovice, Czech Republic). Vanillin and phosphate buffer components (potassium dihydrogen phosphate and disodium hydrogen phosphate) were supplied by Reanal (Budapest, Hungary). Concentrated sulfuric acid (96%) was obtained from Carlo Erba (Milan, Italy). MTT (3-(4,5-dimethylthiazol-2-yl)-2,5-diphenyltetrazolium bromide) was purchased from Carl Roth (Karlsruhe, Germany). LC-MS grade methanol (99.9%) used for mass spectrometry analysis was acquired from VWR (Radnor, PA, USA). Materials related to *Bacillus subtilis* were prepared as described in Section 2.5 and according to the referenced method.

2.2. Collection of the plant material

The leaves of *Myrtus communis* L. were collected in March 2020 from Antakya, Türkiye. The plant material was identified by Assoc. Prof. Dr. Etil Guzelmeric and a voucher specimen (YEF 20012) has been kept at the Herbarium of the Department of Pharmacognosy, Faculty of Pharmacy, Yeditepe University, Istanbul, Türkiye. Air-dried leaves were stored at room temperature.

2.3. Preparation of the sample test solutions

The leaves of *M. communis* were separated from other plant parts and ground into a fine powder. A precise 5-gram of the powdered leaves was weighed and extracted using an ultrasonic bath for 30 min with 50 mL ethanol–H_2O solvent mixture (7:1 *V/V*). After extraction, the mixture was filtered through filter paper, and the extract was evaporated till dryness by using a rotary evaporator (Heidolph, Schwabach, Germany) at 45 °C with decreasing pressure conditions from 250 mbar to 60 mbar. Then, 50 mg/mL stock solutions were prepared by dissolving the extracts in methanol. For TLC–direct bioautography analysis, samples were diluted 10-fold from the stock solution to a final 5 mg/mL concentration.

2.4. TLC analyses

Samples were applied by means of an Automatic TLC Sampler 3 (ATS3, CAMAG, Muttenz, Switzerland) for 1D-TLC separation as 5 mm bands, 8 mm from the bottom and 15 mm from the edge of the plate, while for 2D-TLC as 2 mm bands, 8 mm from the bottom and 11 mm from the edge of the plate. The 1D-TLC developments were performed up to 8 cm in an unsaturated twin-trough chamber (CAMAG) with toluene–ethyl acetate–methanol (6:3:1, *V/V*) or toluene–isopropyl acetate–acetic acid (45:5:1, *V/V*). These separation methods were used in the order written to obtain 2D-TLC chromatograms. After development, the plates were dried in a stream of cold air (5 min) and documented at white light and at UV 254 nm and 365 nm under a UV lamp (CAMAG). Post-chromatographic derivatization was performed by immersing the plates in vanillin-sulfuric acid reagent (40 mg vanillin, 10 mL ethanol, and 200 µL concentrated sulfuric acid; heating at 110 °C for 5 min), followed by heating for 5 min at 110 °C (Advanced Hot Plate, VWR, Debrecen, Hungary) and documented with a digital camera (Cybershot —DSC-HX60, Sony, Neu-Isenberg, Germany) at white light illumination.

2.5. TLC–B. subtilis assay

Prior to the *B. subtilis* assay, the neutralization of the chromatograms developed with acidic mobile phase was carried out by dipping them into a phosphate buffer solution (0.1 M, pH 7.5) for 4 s and drying with a hair-dryer for 5 min. The preparation of *B. subtilis* (strain F1276, a gift from József Farkas, Central Food Research Institute, Budapest, Hungary) bacterial suspensions and the workflow of TLC–*B. subtilis* assay were previously reported in detail [21]. Briefly, the chromatograms were manually dipped into the cell suspension for 8 s, incubated for 2 h at 37 °C (100% humidity, horizontal position in a polypropylene box), and then the bioautograms were visualized by dipping for 1 s into an aqueous solution (1 mg/mL) of MTT vital dye and a further 0.5 h incubation at 37 °C. Viable cells were stained to a produce purplish background, and bright zones indicated the inhibitory effect of antibacterial compounds.

2.6. 2D-TLC–B. subtilis assay–HRMS(/MS)

The *B. subtilis* bioassay enabled the proper positioning of the antibacterial chromatographic zones from a parallel native chromatogram or directly from the bioautogram under the elution head (4 mm × 2 mm) of the TLC-MS interface (CAMAG), that was utilized for elution of analytes from the plates into the HESI-II probe installed at the hybrid quadrupole-orbitrap mass spectrometer (Orbitrap Exploris 120, Thermo Fisher Scientific, Bremen, Germany). To protect the mass spectrometer against particles of the stationary phase, an in-line filter (0.5 µm porosity x 3 mm diameter, Phenomenex, Torrance, CA, USA) was mounted

between the TLC-MS interface and ion source. Methanol was used as the eluent with a flow rate of 0.2 mL/min. Full scan MS spectra were recorded in negative ionization mode in the range of *m/z* 100–1000 with a resolution of 120,000 with lock mass correction. Spray voltage was set to 2 kV, heater and capillary temperature were maintained at 250 °C and 250 °C, respectively, and nitrogen was used as both sheath and auxiliary gas (10 and 5 arbitrary units, respectively), produced by a Peak Scientific gas generator (Genius XE 35, Glasgow, United Kingdom). Target precursor ions were fragmented using a collision energy of 30–45%. Xcalibur software (Version 4.7.69, Thermo Fisher Scientific) was applied to collect and evaluate the data.

3. Results and discussion

3.1. (2D-)TLC–Bacillus subtilis assay

Antibacterial compounds of *M. communis* leaf hydroalcoholic extract were investigated by TLC–*B. subtilis* assay using different applied amounts (2–250 μg) of the extract and two different mobile phase systems: toluene–isopropyl acetate–acetic acid (45:5:1, *V/V*) and toluene–ethyl acetate–methanol (6:3:1, *V/V*). The results demonstrated in Fig. 1 confirmed that the extract contains several major and minor components with antibacterial effects, as evident from the inhibition zones. As the concentration increased, the inhibition zones of the major active compounds expanded, while zones of minor active compounds became visible, leading to the overlapping inhibition zones. To overcome this issue, a 2D-TLC separation method was utilized with the combination of the previously developed mobile phases, which provided improved resolution by reducing zone overlap and enhancing differentiation of compound zones (Figs. 2 and S1). The 2D-TLC–UV/Vis/FLD–*B. subtilis* method allowed for better separation and facilitated the identification of the compounds responsible for bacterial inhibition (Figs. 2 and S1). The 2D-TLC–*B. subtilis* bioautograms demonstrate that the 2D separation of 40 μg of hydroalcoholic extract (Fig. 2A) allowed the visualization of seven major active zones (1–7), while increasing the amount to 250 μg (Fig. 2B) enabled the detection of zones of minor active compounds (8–21) together with major ones.

3.2. 2D-TLC–B. subtilis–HESI–HRMS/MS

The accurate positioning of the elution head (2 × 4 mm) can present a challenge, particularly in cases where no chromatographic zones are visible under UV light (Figure S1) to allow manual marking of the regions of interest. To address this limitation, a parallel-developed chromatogram subjected to chemical derivatization or bioassay can be employed to approximately indicate the relevant zones for subsequent analysis on the native chromatogram. However, in 2D-TLC, even minor variations in chromatographic conditions (e.g., humidity, temperature) may subtly alter zone positions, potentially leading to the improper selection of regions for elution. Therefore, the direct elution of compounds from inhibition zones on the bioautogram was attempted. It is noteworthy, though, that the use of native chromatogram for TLC–MS analysis is recommended as it is not disturbed by a large matrix effect (Fig. 3A). Each zone was eluted from the bioautogram within 0.5 min, and exclusively inhibition zones, devoid of accelerated cells, were collected. Analysis of the total ion chromatogram revealed that signals corresponding to the separated antibacterial compounds were detected within the initial 0.2 min, after which they were replaced by matrix signals for the following 0.3 min (Fig. 3B and C).

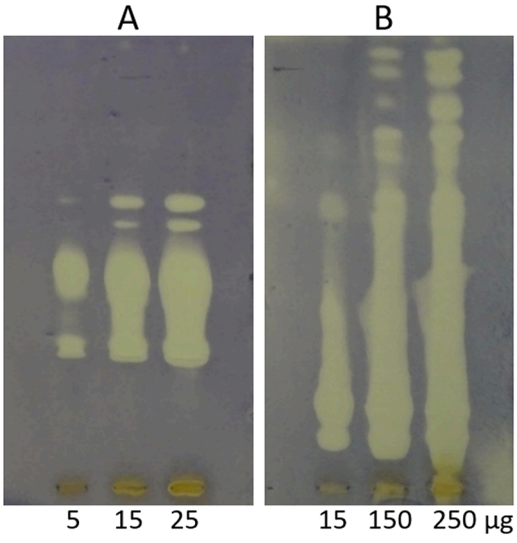

Fig. 1. TLC–*Bacillus subtilis* bioautograms of *Myrtus communis* hydroalcoholic extract developed using (A) toluene–isopropyl acetate–acetic acid (45:5:1, *V/V*) and (B) toluene–ethyl acetate–methanol (6:3:1, *V/V*) mobile phases.

The results of the 2D-TLC–*B. subtilis*–HESI-HRMS/MS analysis of the bioactive zones are presented in Table 1, while the corresponding mass spectra of all detected components are provided in the Supplementary Material (Figures S2-S50). The compounds present in a total of 15 bioactive zones (zones 1, 2, 5–8, and 13–21) were tentatively identified as myrtucommulones or their structural analogues, based on shared molecular ions and characteristic fragmentation patterns in comparison with literature data. In the study conducted by Kashman et al. [30], using MS with electron ionization, the core fragmentation behavior of myrtucommulone derivatives was systematically characterized, with several recurring diagnostic product ions having 182, 196, 250, and 432 molar mass. These ions reflect key structural features of the acylphloroglucinol backbone that is characteristic of myrtucommulone-type compounds. Similarly, a study by Gerbeth et al. [31] revealed that LC–MS/MS analysis in negative ion mode (ESI, $[M–H]^-$) identified a precursor ion at *m/z* 667.4 for myrtucommulone, with the most intense product ion observed at *m/z* 194.9. In addition to this qualifier ion, other characteristic fragments were also reported, including *m/z* 249 and *m/z* 431, which are consistent with typical acylphloroglucinol fragmentation behavior [31]. In the present study, HRMS/MS analysis performed in negative ion mode (HESI, $[M–H]^-$) revealed corresponding product ions in several compounds at *m/z* 181.0870, *m/z* 195.0662, *m/z* 249.1132, *m/z* 415.2124, and *m/z* 431.2073. Among these, *m/z* 181.0870 was the most prominent fragment ion, consistently observed across all zones, and was tentatively assigned to this compound class. The ion at *m/z* 249.1132 is likely to represent a substituted phloroglucinol unit, which constitutes the core structure of myrtucommulone analogues, while the fragment at *m/z* 431.2073 may result from the loss of alkyl side chains from the acylphloroglucinol scaffold. The observed fragmentation pattern, with accurate masses of the product ions aligning closely with previously reported data, provides compelling evidence that the compounds under investigation are myrtucommulone-related natural products. These recurring ions serve as characteristic markers for the tentative identification of myrtucommulone analogues.

Analysis of zone 1 (Figs. 2A and S2) revealed a compound with a characteristic deprotonated molecule at *m/z* 667.3491 $[M–H]^-$ ($C_{38}H_{51}O_{10}^-$). Further HESI–HRMS/MS analysis produced product ions at *m/z* 431.2073, *m/z* 249.1132, *m/z* 195.0662, and *m/z* 181.0870 (Figs. 2C and S3). By comparing the molecular formulae and the fragmentation pattern to literature data, the compound was tentatively identified as myrtucommulone A [30,31]. Zone 2 and zones 16–21 yielded compounds with an identical deprotonated molecule at *m/z* 651.3542 $[M–H]^-$ ($C_{38}H_{51}O_9^-$). Their HRMS/MS fragmentation profile was also identical with signals at *m/z* 469.2594, *m/z* 415.2124, *m/z* 345.1704, and *m/z* 181.0870. Comparing with the previously characterized *M. communis* compounds, the compounds in zones 2 and 16–21 can be tentatively identified as myrtucyclitone B, myrtucyclitone C, myrtucommulone J, or myrtucommuacetalone [32–34] or their constitutional isomers. Zone 6 was detected with a deprotonated molecule at

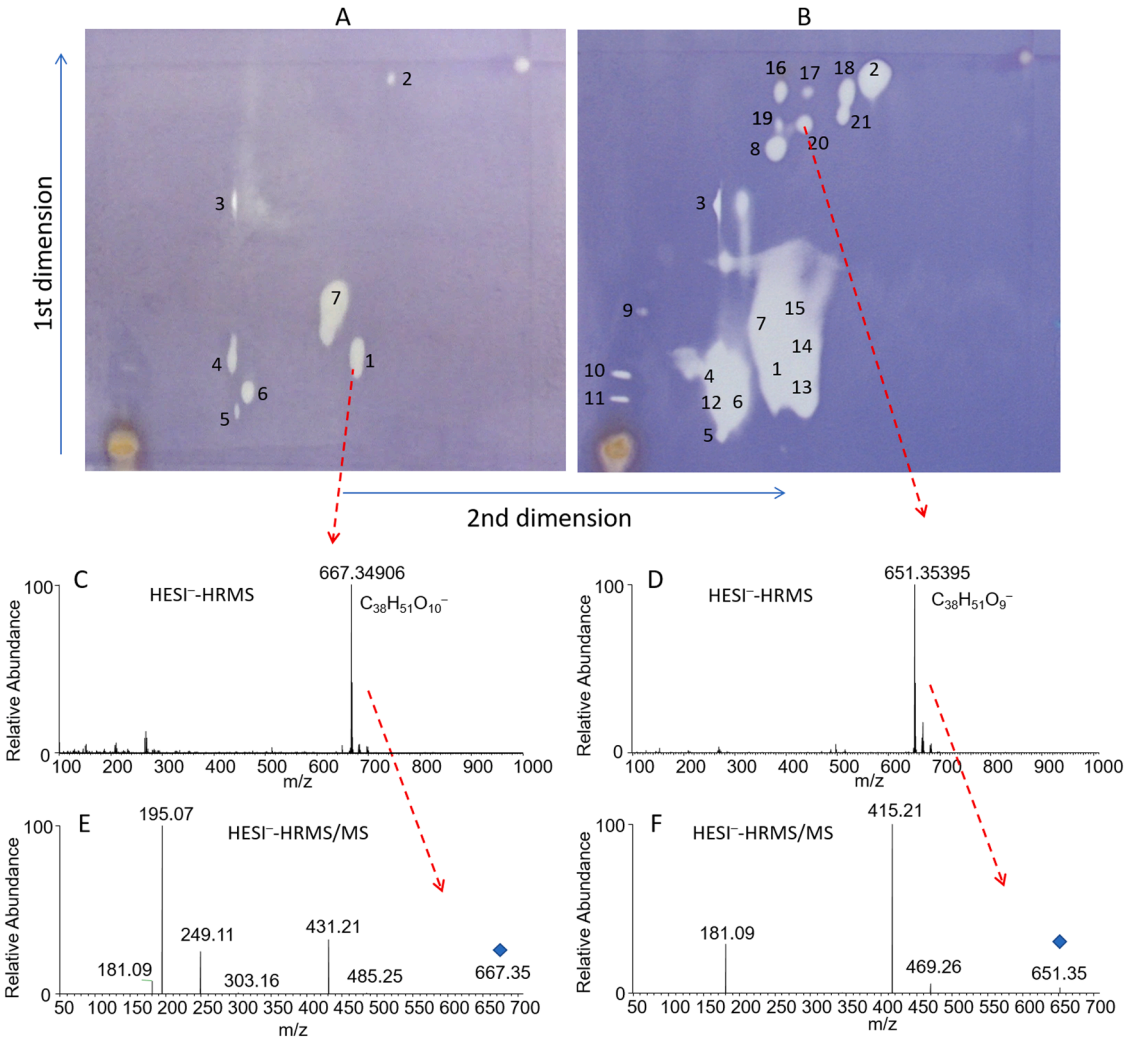

Fig. 2. 2D-TLC–*Bacillus subtilis* bioautograms of (A) 40 μg and (B) 250 μg of *Myrtus communis* hydroalcoholic extract developed in the first dimension with toluene–ethyl acetate–methanol (6:3:1, *V/V*) and in the second dimension with toluene–isopropyl acetate–acetic acid (45:5:1, *V/V*) revealing the inhibition zones 1–21 (bright zones against the bluish background) as well as the 2D-TLC–*B. subtilis*–HESI⁻-HRMS(/MS) spectra of zone 1 (C and E, respectively) and zone 20 (D and F, respectively), obtained via the elution head-based TLC-MS interface.

m/z 431.2048 [M–H]⁻ ($C_{24}H_{31}O_7^-$), and its HRMS/MS analysis revealed fragment ions at *m/z* 249.1133, *m/z* 195.0662, *m/z* 181.0870, *m/z* 151.0764, and *m/z* 125.0245. Molecular formulae led to the tentative identification of the compound as nor–semimyrtucommulone [35]. Compound present in zone 7 provided an intense signal at *m/z* 649.3386 [M–H]⁻ ($C_{38}H_{49}O_9^-$). Its HRMS/MS fragmentation pattern included ions at *m/z* 467.2437, *m/z* 413.1967, *m/z* 343.1548, and *m/z* 181.0870. Based on the parent ion, the compound was tentatively identified as myrtucommulone C and/or myrtucommulone D, previously described in myrtle [8,36,37]. Zone 8 revealed a compound with a deprotonated molecule at *m/z* 413.1965 [M–H]⁻ ($C_{24}H_{29}O_6^-$). Fragment ions at *m/z* 355.1184, *m/z* 337.1082, and *m/z* 297.0495 were recorded in the HRMS/MS spectrum. Molecular formulae and fragment ions support the identification of this compound as myrtucommulone B and/or isomyrtucommulone B [9,30,37]. In the analysis of zone 15 MS signal at *m/z* 663.3544 [M–H]⁻ ($C_{39}H_{51}O_9^-$) was obtained. Its HRMS/MS spectrum displayed major product ions at *m/z* 481.2594, *m/z* 427.2124, *m/z* 413.1969, *m/z* 343.1548, and *m/z* 181.0870, which are characteristic of phloroglucinol derivatives. Based on its molecular formulae, the compound was tentatively identified as myrtucomvalone F and/or callistenone D, both previously reported in *M. communis* and related Myrtaceae species [38,39]. The compounds detected in zones 5 (*m/z* 655.3493, [M–H]⁻, $C_{37}H_{51}O_{10}^-$), 13 (*m/z* 681.3648, [M–H]⁻, $C_{39}H_{53}O_{10}^-$), and 14 (*m/z* 665.3336, [M–H]⁻, $C_{38}H_{49}O_{10}^-$) displayed distinct molecular formulae not directly matched with known myrtucommulone derivatives reported in the literature. However, all three compounds exhibited highly similar fragmentation patterns, including the recurrent detection of fragment ions at *m/z* 181.0870 and *m/z* 195.0663, which are indicative of a phloroglucinol core structure while differences in *m/z* 429.1917 (zone 13) and *m/z* 431.2073 (zone 14), as well as *m/z* 249.1132 (zone 5) and *m/z* 247.0976 (zone 14), suggest structural variations such as a double bond or functional group oxidation. These overlapping fragments suggest the presence of a conserved structural scaffold, despite variations in molecular mass. Collectively, the spectral similarities strongly support the hypothesis that these compounds might represent previously undescribed myrtucommulone analogues with extended or altered side chains.

In addition to the myrtucommulone-related zones, bioactive triterpenoid compounds were also detected in zones 3, 9, and 10. Tentative identification of these compounds was initially performed based on their HRMS spectra and fragmentation profiles. Zone 3 exhibited a deprotonated molecule at *m/z* 455.3529 [M–H]⁻ ($C_{30}H_{47}O_3^-$), with key fragment ions at *m/z* 407.3318, *m/z* 391.3005, and *m/z* 373.2505. These signals are consistent with a pentacyclic triterpenoid structure, and compared with those of the standards, the presence of oleanolic acid and/or ursolic acid are suggested (Figures S7-S9), both previously reported in

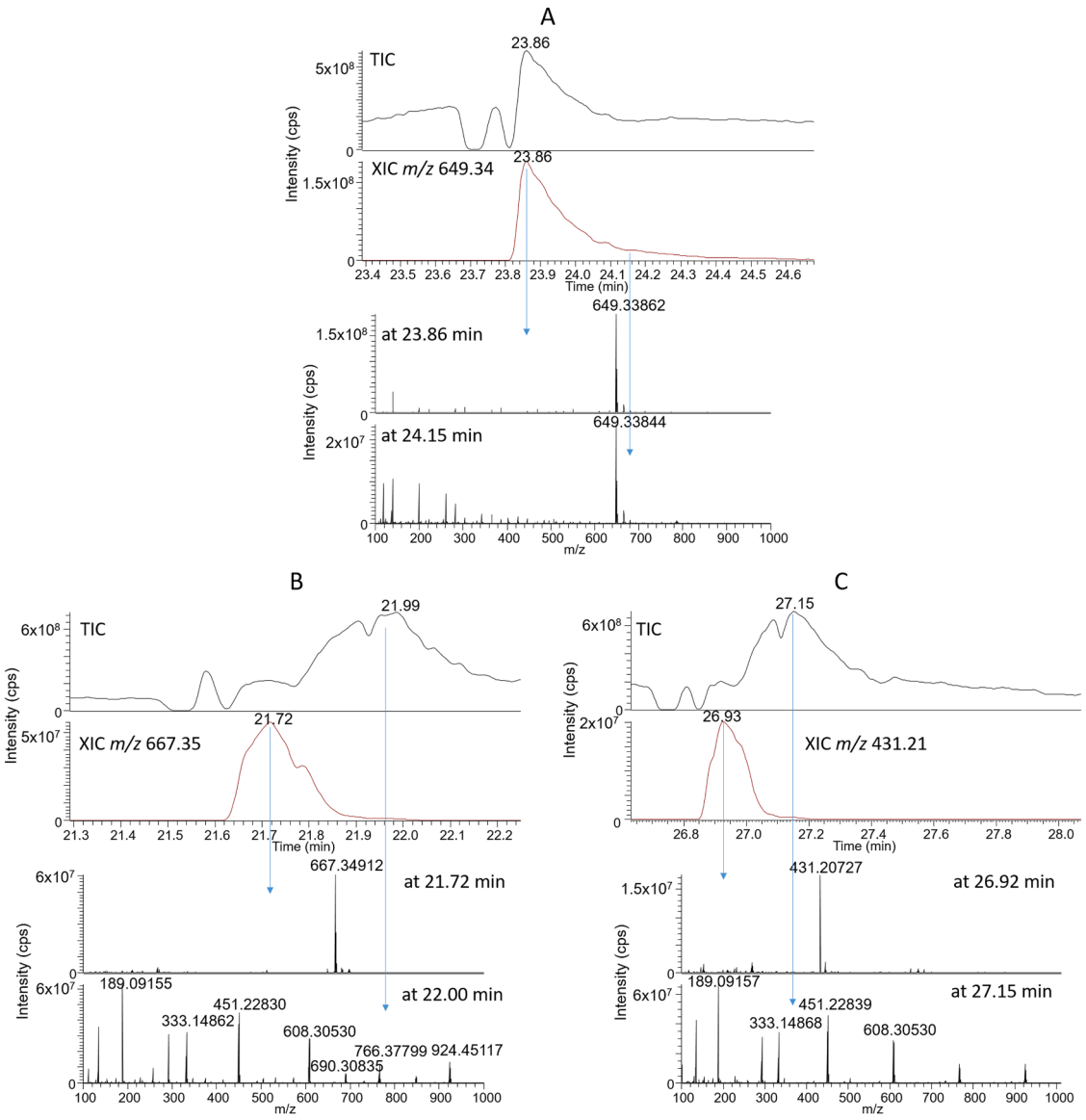

Fig. 3. Total ion chromatograms (TIC), extracted ion chromatograms (XIC), and recorded mass spectra obtained by 2D-TLC–HRMS analysis of zone 7 (A) and 2D-TLC–*Bacillus subtilis*–HRMS analyses of zones 1 and 6 (B and C, respectively).

M. communis [40]. MS signal in zone 9 at *m/z* 471.3477 $[M–H]^-$ ($C_{30}H_{47}O_4^-$), with fragments at *m/z* 423.3244, *m/z* 405.3139, *m/z* 393.3140, and *m/z* 377.2827, identical with that of standards (Figures S22-S24), indicated the likely presence of maslinic acid and/or corosolic acid previously described in myrtle [40]. Due to their high structural similarity, these triterpene pairs (oleanolic and ursolic acids, as well as maslinic and corosolic acids) can only be separated on silica gel following derivatization (Fig. 4) [41]. Moreover, they exhibit identical MS and MS/MS spectra, respectively (Figures S7-S9 and S22-S24), which renders their distinction impossible within the applied analytical system. To support their identification, 1D-TLC and 2D-TLC analyses were performed with *M. communis* hydroalcoholic extract comparing with reference standards of ursolic acid, betulinic acid, oleanolic acid, corosolic acid and maslinic acid. (Fig. 4). The bioactivity of the tentatively identified triterpenoids against *B. subtilis* was assessed using a 1D-TLC bioautography assay (Fig. 4). Following the bioassay, a parallel TLC plate was developed and derivatized with vanillin/sulphuric acid reagent to visualize the corresponding phytochemical spots. By comparing the R_F values, the bioactive zones observed in the *B. subtilis* assay were matched with specific triterpenoid standards, confirming their presence within the myrtle extract. Subsequently, 2D-TLC–vanillin/sulphuric acid analysis of the *M. communis* extract was carried out in an attempt to compare the position of the bioactive zones with authentic standards. This confirmed that zone 3 can correspond to both ursolic and oleanolic acids, while zone 9 matched the R_F values of both maslinic and corosolic acids, thereby supporting their tentative identification.

Compound in zone 10 gave the signal at *m/z* 487.3427 $[M–H]^-$ ($C_{30}H_{47}O_5^-$), accompanied by fragment ions at *m/z* 421.3090, *m/z* 409.3090, *m/z* 391.2984, *m/z* 379.2985, and *m/z* 363.2672. This fragmentation behavior was similar to that of pygenic acid B (Figure S27–28)), thus it supports the tentative identification as triterpenic acid, like pygenic acid B, and/or arjunolic acid, and/or tormentic acid.

In addition to the tentatively identified components, several compounds within the *M. communis* extract remained structurally unresolved. Notably, compounds in zones 4 and 12 exhibited similar fragmentation behavior, suggesting the presence of structurally related constituents. The analysis of zone 4 revealed two distinct compounds with signals of deprotonated molecules at *m/z* 637.3384 ($C_{37}H_{49}O_9^-$) and

Table 1
Substances in antimicrobial zones (1–21) of the *Myrtus communis* leaf extract detected by 2D-TLC–*Bacillus subtilis* bioassay and assigned via 2D-TLC–*B. subtilis*–HESI$^-$-HRMS/MS.

Zones	HRMS signals *m/z* [M–H$^-$]	HCD (%)	HRMS/MS signals *m/z*	Tentative identification
1	667.3491 ($C_{38}H_{51}O_{10}^-$)	30	431.2073 ($C_{24}H_{31}O_7^-$) 249.1132 ($C_{14}H_{17}O_4^-$) 195.0662 ($C_{10}H_{11}O_4^-$) 181.0870 ($C_{10}H_{13}O_3^-$)	Myrtucommulone A [30,31]
2	651.3542 ($C_{38}H_{51}O_9^-$)	30	469.2594 ($C_{28}H_{37}O_6^-$) 415.2124 ($C_{24}H_{31}O_6^-$) 345.1704 ($C_{20}H_{25}O_5^-$) 181.0870 ($C_{10}H_{13}O_3^-$)	Myrtucyclitone B [32] and/or Myrtucyclitone C [32] and/or Myrtucommulone J [33] and/or Myrtucommuacetalone [33] and/or their constitutional isomers
3	455.3529 ($C_{30}H_{47}O_3^-$)	45	407.3318 ($C_{29}H_{43}O^-$) 391.3005 ($C_{28}H_{39}O^-$) 373.2505 ($C_{27}H_{33}O^-$)	Oleanolic acid [40] and/or Ursolic acid [40]
4	637.3384 ($C_{37}H_{49}O_9^-$)	30	567.2963 ($C_{33}H_{43}O_8^-$) 549.2858 ($C_{33}H_{41}O_7^-$) 523.2336 ($C_{30}H_{35}O_8^-$) 495.2386 ($C_{29}H_{35}O_7^-$) 467.2438 ($C_{28}H_{35}O_6^-$) 169.0870 ($C_9H_{13}O_3^-$) 113.0972 ($C_7H_{13}O^-$)	
	639.3547 ($C_{37}H_{51}O_9^-$)	30	569.3119 ($C_{33}H_{45}O_8^-$) 551.3014 ($C_{33}H_{43}O_7^-$) 525.2493 ($C_{30}H_{37}O_8^-$) 497.2544 ($C_{29}H_{37}O_7^-$) 469.2594 ($C_{28}H_{37}O_6^-$) 169.0870 ($C_9H_{13}O_3^-$) 113.0972 ($C_7H_{13}O^-$)	
5	655.3493 ($C_{37}H_{51}O_{10}^-$)	30	473.2544 ($C_{27}H_{37}O_7^-$) 419.2074 ($C_{23}H_{31}O_7^-$) 349.1653 ($C_{19}H_{25}O_6^-$) 305.1031 ($C_{16}H_{17}O_6^-$) 249.1132 ($C_{14}H_{17}O_4^-$) 181.0870 ($C_{10}H_{13}O_3^-$)	Unknown myrtucommulone
6	431.2048 ($C_{24}H_{31}O_7^-$)	30	249.1133 ($C_{14}H_{17}O_4^-$) 195.0662 ($C_{10}H_{11}O_4^-$) 181.0870 ($C_{10}H_{13}O_3^-$) 151.0764 ($C_9H_{11}O_2^-$)	Nor–semimyrtucommulone [35]
7	649.3386 ($C_{38}H_{49}O_9^-$)	30	125.0245 ($C_6H_5O_3^-$) 467.2437 ($C_{28}H_{35}O_6^-$) 413.1967 ($C_{24}H_{29}O_6^-$) 343.1548 ($C_{20}H_{23}O_5^-$) 181.0870 ($C_{10}H_{13}O_3^-$)	Myrtucommulone C [37] and/or Myrtucommulone D [37,36]
8	413.1965 ($C_{24}H_{29}O_6^-$)	35	355.1184 ($C_{20}H_{19}O_6^-$) 337.1082 ($C_{20}H_{17}O_5^-$) 297.0495 ($C_{18}H_{11}O_5^-$)	Myrtucommulone B [9,30,37] and/or Isomyrtucommulone B [9]
9	471.3477 ($C_{30}H_{47}O_4^-$)	45	423.3244 ($C_{29}H_{43}O_2^-$) 405.3139 ($C_{29}H_{41}O^-$) 393.3140 ($C_{28}H_{41}O^-$) 377.2827 ($C_{27}H_{37}O^-$)	Maslinic acid [38] and/or Corosolic acid [38]
10	487.3427 ($C_{30}H_{47}O_5^-$)	45	421.3090 ($C_{29}H_{41}O_2^-$) 409.3090 ($C_{29}H_{43}O^-$) 391.2985 ($C_{28}H_{39}O^-$) 379.2985 ($C_{27}H_{39}O^-$) 363.2672 ($C_{26}H_{35}O^-$)	triterpene pygenic acid B, and/or arjunolic acid and/or tormentic acid
11	no characteristic identifiable signal			
12	681.3284 ($C_{38}H_{49}O_{11}^-$)	30	637.3380 ($C_{37}H_{49}O_9^-$) 549.2857 ($C_{33}H_{41}O_7^-$) 495.2387 ($C_{29}H_{35}O_7^-$) 467.2438 ($C_{28}H_{35}O_6^-$) 277.1081 ($C_{15}H_{17}O_5^-$) 169.0870 ($C_9H_{13}O_3^-$) 113.0972 ($C_7H_{13}O^-$)	
	683.3444 ($C_{38}H_{51}O_{11}^-$)	30	639.3432 ($C_{37}H_{51}O_9^-$) 551.2911 ($C_{33}H_{43}O_7^-$) 497.2449 ($C_{29}H_{37}O_7^-$) 277.1081 ($C_{15}H_{17}O_5^-$) 169.0870 ($C_9H_{13}O_3^-$) 113.0972 ($C_7H_{13}O^-$)	
13	681.3648 ($C_{39}H_{53}O_{10}^-$)	30	445.22286 ($C_{25}H_{33}O_7^-$) 431.2073 ($C_{24}H_{31}O_7^-$) 263.1289 ($C_{15}H_{19}O_4^-$) 209.0819 ($C_{10}H_{13}O_4^-$) 195.0663 ($C_{10}H_{11}O_4^-$)	Unknown myrtucommulone

(*continued on next page*)

Table 1 (*continued*)

Zones	HRMS signals *m/z* [M–H⁻]	HCD (%)	HRMS/MS signals *m/z*	Tentative identification
			181.0870 ($C_{10}H_{13}O_3^-$)	
14	665.3336 ($C_{38}H_{49}O_{10}^-$)	30	495.2387 ($C_{29}H_{35}O_7^-$) 483.2659 ($C_{29}H_{39}O_6^-$) 429.1917 ($C_{24}H_{29}O_7^-$) 359.1497 ($C_{20}H_{23}O_6^-$) 247.0976 ($C_{14}H_{15}O_4^-$) 195.0663 ($C_{10}H_{11}O_4^-$) 181.0870 ($C_{10}H_{13}O_3^-$)	Unknown myrtucommulone
15	663.3544 ($C_{39}H_{51}O_9^-$)	30	481.2594 ($C_{29}H_{37}O_6^-$) 427.2124 ($C_{25}H_{31}O_6^-$) 413.1969 ($C_{24}H_{29}O_6^-$) 343.1548 ($C_{20}H_{23}O_5^-$) 181.0870 ($C_{10}H_{13}O_3^-$)	Myrtucomvalone F [38] and/or Callistenone D [39]
16–21	651.3542 ($C_{38}H_{51}O_9^-$)	30	469.2594 ($C_{28}H_{37}O_6^-$) 415.2124 ($C_{24}H_{31}O_6^-$) 345.1704 ($C_{20}H_{25}O_5^-$) 181.0870 ($C_{10}H_{13}O_3^-$)	Myrtucyclitone B [32] and/or Myrtucyclitone C [32] and/or Myrtucommulone J [33,34, 40] and/or Myrtucommuacetalone [33] and/or their constitutional isomers

m/z 639.3547 ($C_{37}H_{51}O_9^-$), respectively. Both compounds displayed comparable HRMS/MS fragmentation profiles, with shared product ions at *m/z* 549.2858 / 551.3014, *m/z* 495.2386 / 497.2544, and *m/z* 467.2438 / 469.2594, as well as the common diagnostic ions at *m/z* 169.0870 and *m/z* 113.0972. Similarly, zone 12 also contained two structurally related compounds with signals at *m/z* 681.3284 ($C_{38}H_{49}O_{11}^-$) and *m/z* 683.3444 ($C_{38}H_{51}O_{11}^-$), which produced analogous fragmentation patterns. Key shared ions included *m/z* 549.2857 / 551.2911, *m/z* 495.2387 / 497.2449, *m/z* 277.1081, *m/z* 169.0870, and *m/z* 113.0972 mirroring the fragment series observed in zone 4. Despite minor differences in molecular masses and fragment distribution, the overall spectral similarities indicate that these compounds belong to the same structural family. Since no exact matches were found in existing literature, these compounds may represent novel or previously unreported myrtucommulone-type analogues, reflecting the chemical diversity and complexity of the *M. communis* extract. In the case of zone 11, signals of matrix dominated the obtained MS spectrum next to crowded signals with low intensity that prevented any meaningful structural elucidation. This ambiguity is most likely attributable to the co-elution of multiple minor constituents with similar physicochemical properties. As a result, no discrete compound could be confidently assigned to this zone.

4. Conclusion

This study demonstrates that the *M. communis* hydroalcoholic extract contains structurally diverse metabolites with antibacterial activity against Gram-positive *B. subtilis*. The analysis employed a 2D-TLC–UV/Vis/FLD–*B. subtilis* assay–HESI-HRMS/MS eight-dimensional workflow that, to the best of our knowledge, has not previously been applied. The use of 2D-TLC for myrtle leaf extract enabled higher loading of the sample and provided enhanced separation capacity, allowing the detection of both major and minor bioactive zones to be resolved, many of which remain undetected in 1D-TLC systems. By combining bioassay-guided screening with the subsequent HRMS/MS analysis directly from the bioautogram, bioactivity could be directly linked to chemical identities. This approach enabled the tentative identification of fifteen

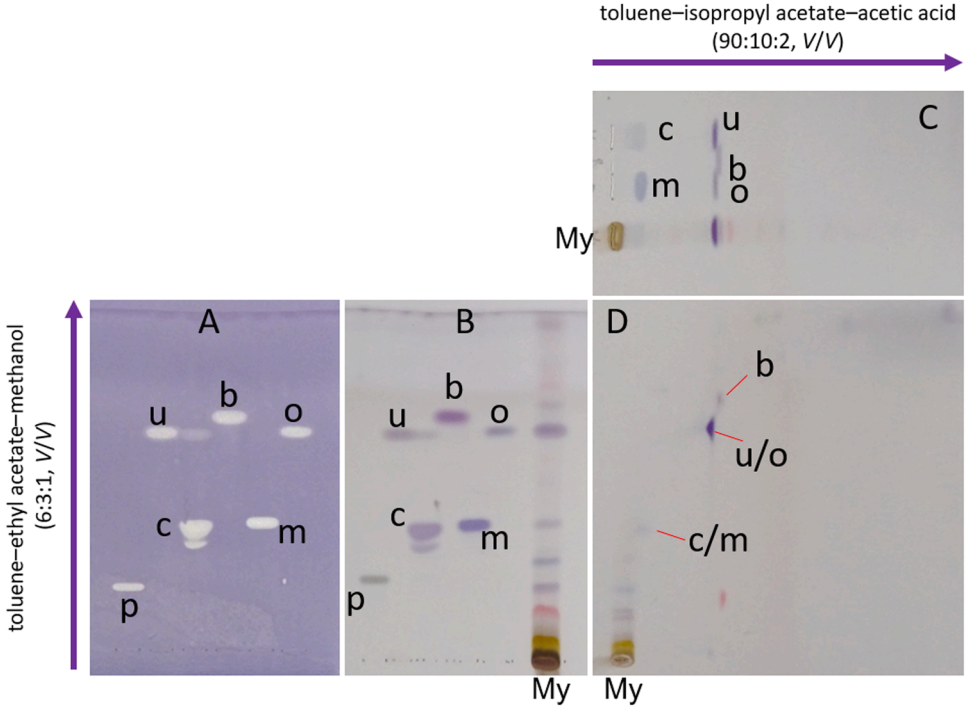

Fig. 4. 1D-TLC (A-C) and 2D-TLC (D) separation of *Myrtus communis* extract (My) and triterpenes ursolic acid (u), betulinic acid (b), oleanolic acid (o), corosolic acid (c), maslinic acid (d), and pygenic acid B (p) using toluene–ethyl acetate–methanol 6:3:1, *V/V* (A, B and first dimension in D) and toluene–isopropyl acetate–acetic acid 45:5:1, *V/V* (C and second dimension in D) mobile phases, and visualized by *Bacillus subtilis* assay (A) or vanillin-sulfuric acid derivatization (B-D).

myrtucommulone-type acylphloroglucinols and several triterpenoids, as well as compounds in multiple antibacterial zones were consistent with novel myrtucommulone analogues, indicating that *M. communis* may harbor previously undescribed natural products of pharmacological relevance.

Overall, this study shows that 2D-TLC–UV/Vis/FLD–bioassay–HRMS/MS can serve as a comprehensive approach for studying complex plant extracts. The method improves resolution, reveals both major and minor bioactive zones, and directly connects bioactivity with chemical identity. Thus, it provides new opportunities for exploring specialized metabolite profiles and supports the discovery of bioactive natural products in complex matrices.

CRediT authorship contribution statement

Ecesu Sezen: Writing – original draft, Investigation, Data curation. **Ágnes M. Móricz:** Writing – review & editing, Supervision, Resources, Methodology, Data curation, Conceptualization. **Péter G. Ott:** Investigation. **Etil Guzelmeric:** Writing – review & editing, Supervision, Resources, Conceptualization.

Declaration of competing interest

The authors declare that they have no known competing financial interests or personal relationships that could have appeared to influence the work reported in this paper.

Acknowledgements

This work was partially funded by the National Research, Development and Innovation Office of Hungary (SNN139496, Á.M.M.).

Supplementary materials

Supplementary material associated with this article can be found, in the online version, at doi:10.1016/j.chroma.2026.466941.

Data availability

Data will be made available on request.

References

[1] M.A. Jabri, L. Marzouki, H. Sebai, Ethnobotanical, phytochemical and therapeutic effects of *Myrtus communis* L. berries seeds on gastrointestinal tract diseases: a review, Arch. Physiol. Biochem. 124 (5) (2018) 390–396, https://doi.org/10.1080/13813455.2017.1423504.

[2] A. Dafni, Myrtle (*Myrtus communis*) as a ritual plant in the Holy Land—A comparative study in relation to ancient traditions, Econ. Bot. 70 (2016) 222–234.

[3] A.E. Al-Snafi, J.O. Teibo, H.M. Shaheen, O.A. Akinfe, T.K.A. Teibo, N. Emieseimokumo, G.E.S. Batiha, The therapeutic value of *Myrtus communis* L.: an updated review, Naunyn-Schmiedeberg's Arch. Pharmacol. 397 (2024) 1–22, https://doi.org/10.1007/s00210-024-03019-8.

[4] G. Alipour, S. Dashti, H. Hosseinzadeh, Review of pharmacological effects of *Myrtus communis* L. and its active constituents, Phytother. Res. 28 (2014) 1125–1136, https://doi.org/10.1002/ptr.5118.

[5] E. Guzelmeric, P. Ugurlu, C. Celik, N.B. Sen, S. Helvacioglu, M. Charehsaz, E. Yesilada, *Myrtus communis* L. (Myrtle) plant parts: comparative assessment of their chemical compositions and antioxidant, anticancer, and antimutagenic activities, S. Afr. J. Bot. 150 (2022) 711–720, https://doi.org/10.1016/j.sajb.2022.06.034.

[6] O. Celaj, A.G. Duran, P. Cennamo, M. Scognamiglio, A. Fiorentino, A. Esposito, B. D'Abrosca, Phloroglucinols from Myrtaceae: attractive targets for structural characterization, biological properties and synthetic procedures, Phytochem. Rev. 20 (2021) 259–299, https://doi.org/10.1007/s11101-020-09708-y.

[7] V. Aleksic, P. Knezevic, Antimicrobial and antioxidative activity of extracts and essential oils of *Myrtus communis* L, Microbiol. Res. 169 (2014) 240–254, https://doi.org/10.1016/j.micres.2013.10.003.

[8] R. Nicoletti, M.M. Salvatore, P. Ferranti, A. Andolfi, Structures and bioactive properties of myrtucommulones and related acylphloroglucinols from Myrtaceae, Molecules 23 (2018) 3370, https://doi.org/10.3390/molecules23123370.

[9] G. Appendino, F. Bianchi, A. Minassi, O. Sterner, M. Ballero, S. Gibbons, Oligomeric acylphloroglucinols from myrtle (*Myrtus communis*), J. Nat. Prod. 65 (2002) 334–338, https://doi.org/10.1021/np010405u.

[10] Á.M. Móricz, P.G. Ott, T.T. Häbe, A. Darcsi, A. Böszörményi, Á. Alberti, D. Krüzselyi, P. Csontos, S. Béni, G.E. Morlock, Effect-directed discovery of bioactive compounds followed by highly targeted characterization, isolation and identification, exemplarily shown for *Solidago virgaurea*, Anal. Chem. 88 (2016) 8202–8209, https://doi.org/10.1021/acs.analchem.6b02007.

[11] Á.M. Móricz, D. Szeremeta, M. Knaś, E. Długosz, P.G. Ott, T. Kowalska, M. Sajewicz, Antibacterial potential of the *Cistus incanus* L. phenolics as studied with use of thin-layer chromatography combined with direct bioautography and in situ hydrolysis, J. Chromatogr. A 1534 (2018) 170–178, https://doi.org/10.1016/j.chroma.2017.12.056.

[12] G. Yüce, G.E. Morlock, Streamlined structure elucidation of an unknown compound in a pigment formulation, J. Chromatogr. A 1469 (2016) 120–127, https://doi.org/10.1016/j.chroma.2016.09.040.

[13] F. Rabel, J. Sherma, A review of advances in two-dimensional thin-layer chromatography, J. Liq. Chromatogr. Relat. Technol. 39 (2016) 627–639, https://doi.org/10.1080/10826076.2016.1214844.

[14] L. Stütz, S.C. Weiss, W. Schulz, W. Schwack, R. Winzenbacher, Selective two-dimensional effect-directed analysis with thin-layer chromatography, J. Chromatogr. A 1524 (2017) 273–282, https://doi.org/10.1016/j.chroma.2017.10.009.

[15] Á.M. Móricz, T.T. Häbe, P.G. Ott, G.E. Morlock, Comparison of high-performance thin-layer with overpressured layer chromatography combined with direct bioautography and direct analysis in real time mass spectrometry for tansy root, J. Chromatogr. A 1603 (2019) 355–360, https://doi.org/10.1016/j.chroma.2019.03.068.

[16] C. Cimpoiu, V. Miclaus, G. Damian, M. Puia, D. Casoni, C. Bele, T. Hodisan, Identification of new phthalazine derivatives by HPTLC-FTIR and characterization of their separation using some molecular properties, J. Liq. Chromatogr. Relat. Technol. 26 (2006) 2687–2696, https://doi.org/10.1081/JLC-120024538.

[17] Á.M. Móricz, E. Horváth, P.G. Ott, E. Tyihák, Raman spectroscopic evaluation of the influence of *Pseudomonas* bacteria on aflatoxin B₁ in the BioArena complex bioautographic system, J. Raman Spectrosc. 39 (2008) 1332–1337, https://doi.org/10.1002/jrs.1998.

[18] S. Agatonovic-Kustrin, G. Ramenskaya, E. Kustrin, D. Babazadeh Ortakand, D. W. Morton, A new integrated HPTLC-ATR/FTIR approach in marine algae bioprofiling, J. Pharm. Biomed. Anal. 189 (2020) 113488, https://doi.org/10.1016/j.jpba.2020.113488.

[19] E. Azadniya, G.E. Morlock, Bioprofiling of *Salvia miltiorrhiza* via planar chromatography linked to (bio)assays, high resolution mass spectrometry and nuclear magnetic resonance spectroscopy, J. Chromatogr. A 1533 (2018) 180–192, https://doi.org/10.1016/j.chroma.2017.12.014.

[20] E.M. Grzelak, C. Hwang, G. Cai, J.-W. Nam, M.P. Choules, W. Gao, D.C. Lankin, J. B. McAlpine, S.G. Mulugeta, J.G. Napolitano, J.-W. Suh, S.H. Yang, J. Cheng, H. Lee, J.-Y. Kim, S.-H. Cho, G.F. Pauli, S.G. Franzblau, B.U. Jaki, Bioautography with TLC-MS/NMR for rapid discovery of anti-tuberculosis lead compounds from natural sources, ACS Infect. Dis. 2 (2016) 294–301, https://doi.org/10.1021/acsinfecdis.5b00150.

[21] Á.M. Móricz, T.T. Häbe, A. Böszörményi, P.G. Ott, G.E. Morlock, Tracking and identification of antibacterial components in the essential oil of *tanacetum vulgare* L. by the combination of high-performance thin-layer chromatography with direct bioautography and mass spectrometry, J. Chromatogr. A 1422 (2015) 310–317, https://doi.org/10.1016/j.chroma.2015.10.010.

[22] Á.M. Móricz, P.G. Ott, G.E. Morlock, Discovered acetylcholinesterase inhibition and antibacterial activity of polyacetylenes in tansy root extract via effect-directed chromatographic fingerprints, J. Chromatogr. A 1543 (2018) 73–80, https://doi.org/10.1016/j.chroma.2018.02.038.

[23] S.P. Pasilis, V. Kertesz, G.J. Van Berkel, M. Schulz, S. Schorcht, Using HPTLC/DESI-MS for peptide identification in 1D separations of tryptic protein digests, Anal. Bioanal. Chem. 391 (2008) 317–324, https://doi.org/10.1007/s00216-008-1874-6.

[24] M. Jamshidi-Aidji, G.E. Morlock, From bioprofiling and characterization to bioquantification of natural antibiotics by direct bioautography linked to high-resolution mass spectrometry: exemplarily shown for *Salvia miltiorrhiza* root, Anal. Chem. 88 (2016) 10979–10986, https://doi.org/10.1021/acs.analchem.6b02648.

[25] A. Reguigui, P.G. Ott, A. Darcsi, J. Bakonyi, M. Romdhane, Á.M. Móricz, Nine-dimensional bioprofiles of Tunisian sages (*Salvia officinalis, S. aegyptiaca* and *S. verbenaca*) by high-performance thin-layer chromatography — Effect-directed analyses, J. Chromatogr. A 1688 (2023) 463704, https://doi.org/10.1016/j.chroma.2022.463704.

[26] T.T. Häbe, M. Jamshidi-Aidji, J. Macho, G.E. Morlock, Direct bioautography hyphenated to direct analysis in real time mass spectrometry: chromatographic separation, bioassay and mass spectra, all in the same sample run, J. Chromatogr. A 1568 (2018) 188–196, https://doi.org/10.1016/j.chroma.2018.07.002.

[27] G.E. Morlock, Chromatography combined with bioassays and other hyphenations — The direct link to the compound indicating the effect. Instrumental Methods for the Analysis and Identification of Bioactive Molecules, 2014, https://doi.org/10.1021/bk-2014-1185.ch005. ACS Symp. Ser. 1185ch. 005.

[28] S. Kirchert, G.E. Morlock, Orthogonal hyphenation of planar and liquid chromatography for mass spectrometry of biomarkers out of the bioassay matrix (NP-HPTLC-UV/vis/FLD-Bioassay-RP/IEX-HPLC-UV/vis-ESI-MS), Anal. Chem. 92 (2020) 9057–9064, https://doi.org/10.1021/acs.analchem.0c01251.

[29] T. Schreiner, G.E. Morlock, Non-target bioanalytical eight-dimensional hyphenation including bioassay, heart-cut trapping, online desalting, orthogonal

separations and mass spectrometry, J. Chromatogr. A 1647 (2021) 462154, https://doi.org/10.1016/j.chroma.2021.462154.
[30] Y. Kashman, A. Rotstein, A. Lifshitz, The structure determination of two new acylphloroglucinols from *Myrtus communis* L, Tetrahedron 30 (1974) 991–997, https://doi.org/10.1016/S0040-4020(01)97486-1.
[31] K. Gerbeth, J. Meins, O. Werz, M. Schubert-Zsilavecz, M. Abdel-Tawab, Determination of myrtucommulone from *Myrtus communis* in human and rat plasma, Planta Med. 77 (05) (2011) 450–454, https://doi.org/10.1055/s-0030-1250459.
[32] Y. Wu, J.W. Liu, C. Liu, X.J. Huang, N.P. Li, W.C. Ye, L. Wang, Antibacterial triketone-phloroglucinol-triketone adducts from *Myrtus communis*, Chem. Biodivers. 17 (2020) e2000708, https://doi.org/10.1002/cbdv.202000708.
[33] H. Liu, L. Huo, B. Yang, Y. Yuan, W. Zhang, Z. Xu, H. Tan, Biomimetic-inspired syntheses of myrtucommuacetalone and myrtucommulone J, Org. Lett. 19 (2017) 4786–4789, https://doi.org/10.1021/acs.orglett.7b02291.
[34] F. Cottiglia, L. Casu, M. Leonti, P. Caboni, C. Floris, B. Busonera, P. Farci, A. Ouhtit, G. Sanna, Cytotoxic phloroglucinols from the leaves of *Myrtus communis*, J. Nat. Prod. 75 (2012) 1883–1888, https://doi.org/10.1021/np300368r.
[35] M. Charpentier, M. Hans, J. Jauch, Enantioselective synthesis of myrtucommulone A, Eur. J. Org. Chem. (19) (2013) 4078–4084, https://doi.org/10.1002/ejoc.201300284.
[36] R. Nicoletti, P. Ferranti, S. Caira, G. Misso, M. Castellano, G. Di Lorenzo, M. Caraglia, Myrtucommulone production by a strain of *neofusicoccum australe* endophytic in myrtle (*Myrtus communis*), World J. Microbiol. Biotechnol. 30 (2014) 1047–1052, https://doi.org/10.1007/s11274-013-1523-x.
[37] F. Shaheen, M. Ahmad, S. Nahar Khan, S. Hussain, S. Anjum, B. Tashkhodjaev, K. Turgunov, M.N. Sultankhodzhaev, M.I. Choudhary, Atta-ur-Rahman, new α-glucosidase inhibitors and antibacterial compounds from *Myrtus communis*, Eur. J. Org. Chem. 10 (2006) 2371–2377, https://doi.org/10.1002/ejoc.200500936.
[38] Y. Wu, M. Chen, W.J. Wang, N.P. Li, W.C. Ye, L. Wang, Phloroglucinol derivatives from *Myrtus communis* 'Variegata' and their antibacterial activities, Chem. Biodivers. 17 (2020) e2000292, https://doi.org/10.1002/cbdv.202000292.
[39] M.Y. Yu, S.N. Liu, H. Liu, Q.H. Meng, X.J. Qin, H.Y. Liu, Acylphloroglucinol trimers from *Callistemon salignus* seeds: isolation, configurational assignment, hAChE inhibitory effects, and molecular docking studies, Bioorg. Chem. 117 (2021) 105404, https://doi.org/10.1016/j.bioorg.2021.105404.
[40] C. Liang, D. Staerk, K.T. Kongstad, Potential of *Myrtus communis* Linn. As a bifunctional food: dual high-resolution PTP1B and α-glucosidase inhibition profiling combined with HPLC-HRMS and NMR for identification of antidiabetic triterpenoids and phloroglucinol derivatives, J. Funct. Foods 64 (2020) 103623, https://doi.org/10.1016/j.jff.2019.103623.
[41] Á.M. Móricz, P.G. Ott, Separation and detection of apricot leaf triterpenes by high-performance thin-layer chromatography combined with direct bioautography and mass spectrometry, J. Chromatogr. A 1675 (2022) 463167, https://doi.org/10.1016/j.chroma.2022.463167.